

University of Twente

Faculty of Science and Technology
Soft Matter, Fluidics and Interfaces

Immobilization of TiO_2

Via different routes for photocatalytic reactions in a PDMS based
microreactor

A thesis submitted for the degree of
Bachelor of Science

Presented by Justin Schäffer

j.w.schaffer@student.utwente.nl

Examination Committee

Prof. dr. Ir. R.G.H. Lammertink

MSc. D. Rafieian

Dr. B.A. Boukamp

August, 2012

1 Table of Contents

1	Table of Contents	2
2	Abstract	4
3	Introduction.....	5
4	Theoretical Background.....	6
4.1	Photocatalysis.....	6
4.2	Titanium dioxide.....	7
4.2.1	Reaction Processes	7
4.2.2	Crystal Structures	8
4.2.3	Immobilization.....	10
4.3	Effect of pH and steric stabilization on colloidal stability	11
4.4	Microreactors	13
4.5	Analysis.....	14
4.5.1	UV spectroscopy.....	14
4.5.2	Scanning Electron Microscopy	14
4.5.3	Tape testing.....	15
5	Experimental	16
5.1	TiO ₂ immobilization	16
5.2	Fabrication of the microreactor	18
5.3	Analysis.....	19
5.3.1	Scanning Electron Microscope	19
5.3.2	Tape testing.....	19
5.3.3	Photocatalytic activity	20
6	Results and Discussion	21
6.1	Immobilization.....	21
6.1.1	Pipetted samples	21
6.1.2	Spin coated samples.....	22
6.2	Microreactor fabrication	24
6.3	Photocatalytic activity	24
6.3.1	Calibration	24
6.3.2	Methylene Blue degradation.....	25
7	Conclusions and recommendations	27
7.1	General conclusions	27
7.2	Recommendations.....	28

8	References	29
9	Acknowledgements	30
	Appendix A: Sample overview	31
	Appendix B: SEM images	33

2 Abstract

In this study thin films of TiO_2 were coated on silicon substrates by pipetting or spin coating from a colloidal suspension of Previously Made Titania Powder (PMTP). Influence of sintering temperature, steric stabilization, pH of the suspension, spin coating settings and P25 concentration on surface morphology, film quality and mechanical stability were analyzed by Scanning Electron Microscopy (SEM) and tape testing. Spin coated samples using a higher concentration of PVA (steric stabilizer) and sintered at 500-600 °C resulted in the most uniform, well-covered and mechanically stable films and were applied to a microreactor in which a coated silicon substrate was bound to a PDMS chip containing the microchannel. Dimensions of the channel were: 250 μm (Width) x 150 μm (Depth), 18 mm (Length) and a volume of 0.675 μL . The microreactor was used for photodegradation of Methylene Blue as the model compound under UV illumination. Degradation of up to 51.14% was achieved at a flowrate of 1 $\mu\text{l/min}$.

3 Introduction

The role of catalyst in photocatalytic reactions for removing organic impurities in water is of paramount importance. TiO_2 attracts much attention and is studied widely recently as the desired material due to its various appealing characteristics. Chemically and biologically inertness, relatively convenient production methods, without risks to environment or humans and stability in photocatalytic reactions are only a few factors to mention. ^[1, 5, 6]

TiO_2 photocatalysts are used in different applications such as self cleaning surfaces, water purification, air purification, anticorrosion applications and photocatalytic lithography. This study will focus on the application of TiO_2 for photodegradation of organic compounds. Macroscale systems involving a suspension of TiO_2 powder in aqueous solution which is exposed to UV light are well documented. This type of reactor provides a large surface area but problems arise in the removal of the catalyst from the yield. ^[7]

The separation step is severe and expensive but may be eliminated by the use of an immobilized catalyst resulting in lower operating costs. Many different routes of immobilization on many different substrates have been investigated. Substrates include glass, silica gel, metal, ceramics, polymer, thin films, fibres, zeolite, alumina clays, activated carbon, cellulose, reactor walls and others, and a deposition method that has gained a lot of attention is the sol-gel process. ^[8] Film characteristics of importance include thickness, porosity, strength, and specific surface area.

Although an immobilized catalyst might provide a cheaper solution compared to a suspended catalyst, immobilization does result in a loss of surface area and mass transfer limitations. ^[9] Application of TiO_2 in a microreactor has not been as well-documented as the macroscale systems, but has many advantageous characteristics such as a high surface to volume ratio, laminar flow and short diffusion distances and will therefore receive attention in this work. ^[10, 11]

The aims of this study were:

- Evaluating different routes of TiO_2 immobilization with special emphasis on finding recipes that are compatible with microreactor fabrication.

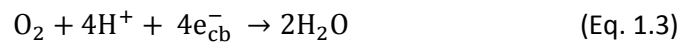
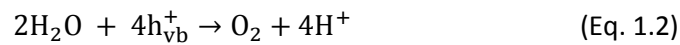
- Application of the compatible recipes in a microreactor and analysis of their photocatalytic activity.

A colloidal suspension of Previously Made Titania Powder (PMTP) was deposited on silicon substrates by two techniques: pipetting and spin coating. Influence of sintering temperature, steric stabilization, pH of the suspension, spin coating settings and P25 concentration on surface morphology, film quality and mechanical stability were analyzed by Scanning Electron Microscopy (SEM) and tape testing. Microreactors incorporating the most favorable recipes were made using different binding techniques used for analysis of the film's photocatalytic activity by degradation of methylene blue as model compound.

4 Theoretical Background

4.1 Photocatalysis

Photocatalysis can be described as a reaction which involves the use of a photocatalyst, often a semiconductor. Absorption of light on the photocatalyst surface creates electron holes (h_{vb}) and a free electrons (e_{cb}) (Eq. 1.1). The most general catalytic reaction consists of an oxidation from the hole (Eq. 1.2) and a reduction from the free electron (Eq. 1.3).^[1]



Generation of free radicals and the electron holes on the surface of the catalyst provides good capabilities to oxidize for example organic pollutants.

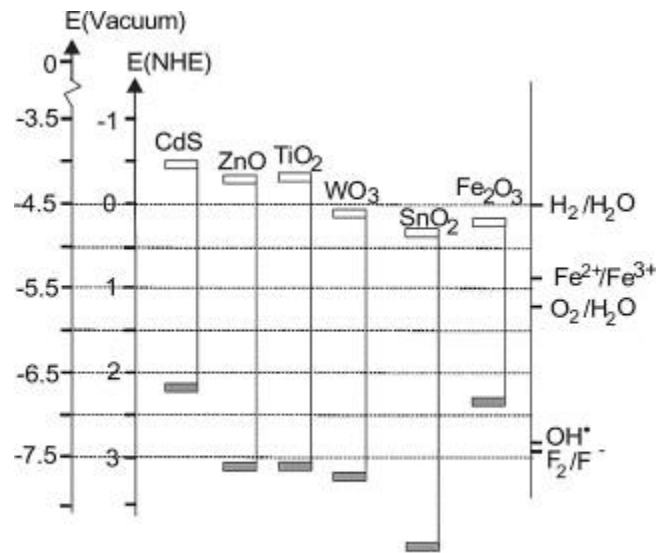


Figure 1. Position of valance (top) and conduction (bottom) band for several semiconductors including TiO₂.^[5]

In order to generate a free electron and electron hole the band gap (bg) of the semi-conductor must be bridged. Incident light must therefore provide sufficient energy to excite an electron from the valence band (vb) to the conduction band (cb). The energy (E) supplied by a photon is given by:

$$E = \frac{hc}{\lambda} \quad (\text{Eq. 1.4})$$

With h the Planck constant, c the speed of light and λ the wavelength of the photon.

For TiO₂ the band gap is 3.0 eV for rutile and 3.2 eV for Anatase, corresponding to a wavelength of 414 nm and 388 nm respectively.^[5]

4.2 Titanium dioxide

4.2.1 Reaction Processes

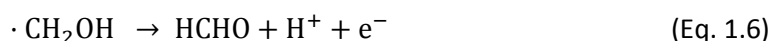
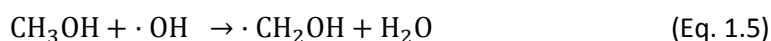
Four primary processes occur on the TiO₂ surface when irradiated with UV-light. These processes and their characteristic times are shown in figure 1. Charge-carrier trapping and interfacial charge transfer are favorable processes for photocatalytic reactions but these compete with charge-carrier recombination. Increase of the charge-carrier lifetime or the increase of the interfacial charge transfer rate result in higher reaction efficiencies. ^[12]

Primary Process	Characteristic Times
Charge-carrier generation $\text{TiO}_2 + h\nu \rightarrow h_{\text{vb}}^+ + e_{\text{cb}}^-$	Fast (fs)
Charge-carrier trapping $h_{\text{vb}}^+ + \text{Ti}^{\text{IV}}\text{OH} \rightarrow \{>\text{Ti}^{\text{IV}}\text{OH} \cdot\}^+$ $e_{\text{cb}}^- + \text{Ti}^{\text{IV}}\text{OH} \leftrightarrow \{>\text{Ti}^{\text{III}}\text{OH}\}$ $e_{\text{cb}}^- + \text{Ti}^{\text{IV}} \rightarrow \text{Ti}^{\text{III}}$	Fast (10 ns) Shallow trap (100 ps) Deep trap (10 ns)
Charge-carrier recombination $e_{\text{cb}}^- + \{>\text{Ti}^{\text{IV}}\text{OH} \cdot\}^+ \rightarrow >\text{Ti}^{\text{IV}}\text{OH}$ $h_{\text{vb}}^+ + \{>\text{Ti}^{\text{III}}\text{OH}\} \rightarrow \text{Ti}^{\text{IV}}\text{OH}$	Slow (100 ns) Fast (10 ns)
Interfacial charge transfer $\{>\text{Ti}^{\text{IV}}\text{OH} \cdot\}^+ + \text{Red} \rightarrow >\text{Ti}^{\text{IV}}\text{OH} + \text{Red}^+$ $e_{\text{tr}}^- + \text{Ox} \rightarrow \text{Ti}^{\text{IV}}\text{OH} + \text{Ox}^-$	Slow (100 ns) Very slow (ms)

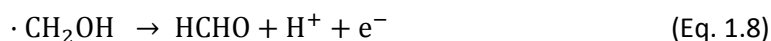
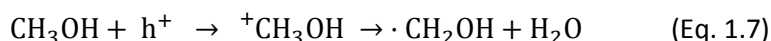
Table 1. Primary processes and their characteristic times ^[12]

Important oxidants generated on the TiO₂ surface include the electron holes, ·OH radicals, O₂^{·-} and ¹O₂. These oxidants may oxidize different organic compounds through different mechanisms. ^[1]

Oxidation of methanol for example may be oxidized by ·OH radicals (indirect oxidation):



Oxidation from the electron holes yields the same reaction products:



However, electron hole lifetime is short and this pathway is only efficient if electron donors and acceptors are readily available at the catalyst surface. In aqueous environment methanol is not available at high concentrations at the TiO₂ surface as the adsorption equilibrium is more in favor of water. Therefore direct oxidation is more likely to be dominant. Formic acid on the other hand shows strong interaction with TiO₂ and is more likely to follow direct oxidation. ^[13, 14]

4.2.2 Crystal Structures

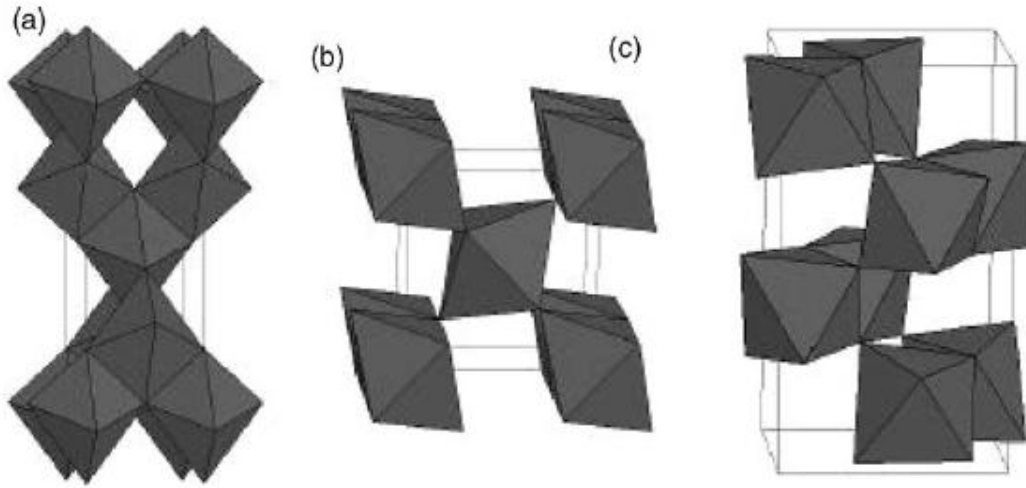


Figure 2. Crystal structures of TiO_2 : Anatase (a), Rutile (b), Brookite (c) ^[5]

TiO_2 crystal structures can be distinguished in three forms: anatase, rutile and brookite. Anatase and rutile structures have been most used in practical work as brookite is rarer and more difficult to prepare. Anatase is dominant at smaller particle sizes (<11 nm) or lower sintering temperatures (<600 °C). Rutile is dominant at bigger particle sizes (>35 nm) or higher sintering temperatures (>600 °C). ^[1, 9, 15, 16] Although rutile has a lower bandgap (anatase: 3.2 eV, rutile: 3.0 eV), anatase shows a higher photocatalytic activity in the oxidation of organic pollutants. ^[17, 18] A precise reason for anatase's better photocatalytic activity has not been documented, but an explanation may be found in anatase's conduction band energy (E_{cb}). Figure 3 shows anatase's E_{cb} to be 0.2 V more negative than rutile's E_{cb} which allows for a more favorable reduction of O_2 to O_2^- over a wide pH range. ^[1]

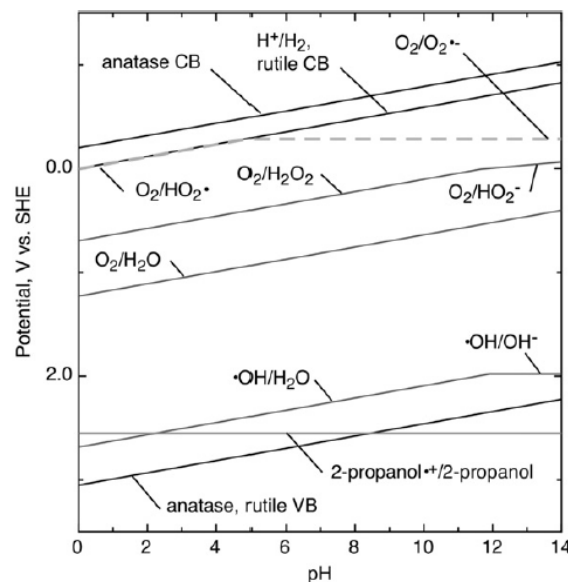


Figure 3. TiO_2 energy bands and corresponding potential differences of redox reactions occurring on the TiO_2 surface as function of PH. ^[1]

Conversion from anatase to rutile may occur but is very slow at room temperature. At higher temperatures however, conversion rate is higher and influenced by different factors. Lattice and surface defects act as nucleation sites and enhance the conversion rate to rutile. As rutile is a more compact structure compared to anatase, occupying approximately 8% less volume, vacancies in the structure also accelerate the process.

The critical nucleus size of rutile particles is much larger than anatase, but anatase particles can sinter together to reach this size. Agglomeration of anatase particles may be prevented by the use of suitable techniques, dispersion on a support or addition of certain compounds. Once the critical nucleus size has been reached, notable conversion to rutile starts at temperatures of 400 °C.^[5]

4.2.3 Immobilization

In current reactor designs either a TiO_2 slurry or immobilized film is used. In the slurry reactors, suspended small TiO_2 particles such as commercially available Aeroxide P25 can have a high surface to volume ratio. However, the suspended particles contaminate the yield and need to be removed. This is more difficult for smaller particles as they stay suspended in water easily, clog filter membranes and penetrate filter materials.^[13] The filtering of the slurry is not practical and comes with an economic cost.

To avoid the filtering process and to increase catalyst durability, TiO_2 catalysts have been successfully immobilized on solid supports as bound particles or thin films. However, the photocatalytic activity of immobilized films is often lower due to a lower surface area to volume ratio and mass transfer limitations.^[19]

Commonly used substrates are glass, activated carbon, silica gel and various polymeric materials and metals. Important properties of the substrate are a good adhesion of the TiO_2 particles, resistance against sintering temperatures, a high specific surface area and strong absorbance affinity towards the pollutants. Glass and silica substrates may be wanted because they are transparent. Activated carbon is very porous and has a very high specific surface area and has shown to increase the activity of the catalyst.^[8]

To deposit the titanium dioxide on the substrate, different techniques may be utilized. The Sol-Gel method has been extensively reported as low cost and easy. This method involves a colloidal suspension of the TiO_2 particles. In the process the suspension is converted to a viscous gel and finally to a solid material. Sol-Gel shows good adherence to the substrate because of oxygen bridges that are formed during heating of the precursor (such as titanium tetrachloride). Dip or spread coating can be used to coat the substrate. Dip coating results in a thin and controllable layer while spread coating may be used to attain a thicker layer.

Another easy and reproducible technique is the use of Previously Made Titania Powder (PMTP).^[9] Unlike the Sol-Gel method which uses a precursor, commercially available titania powder such as Aeroxide P25 is used and mixed with a solvent. Coating may be done by different methods such as pipetting and spin coating. After sintering at high temperature (400-600 °C) the film will adhere to the substrate.

Chemical vapor deposition (CVD) covers a lot of different processes that differ by type of precursor, type of support, uniformity of the film and reaction conditions. The method generally involves exposing the substrate to a volatile gaseous phase precursor in an inert, high temperature and pressure environment. The precursor will decompose at the surface, forming the TiO_2 film. This method can coat a substrate of any shape. Other deposition techniques include sputtering, thermal treatment and electrophoretic deposition.^[8, 9]

4.3 Effect of pH and steric stabilization on colloidal stability

Attractive and repulsive forces in a colloidal suspension may give rise to aggregation of lyophobic colloids. Aggregation is caused by attractive van der Waals forces and occurs when there is a decrease in the overall potential energy when two particles approach. For the lyophobic colloids it is more favorable to be in an aggregated state. However, the repulsive forces caused by interaction of similarly charged electrical double layers create an energy barrier that must be bridged for agglomeration to occur. They are in a so-called metastable state.^[4]

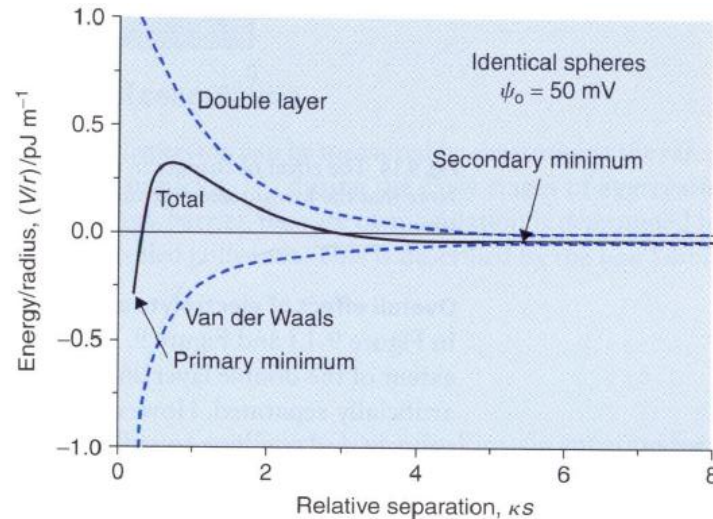


Figure 4. Attractive and repulsive interaction, showing the energy barrier of two approaching particles. ^[4]

The van der Waals forces originate from surface charges on the colloids. Metal oxides such as TiO_2 can form $\text{M} - \text{O}^-$ or $\text{M} - \text{OH}_2^+$, depending on pH. The extent of ionization is indicated by the zeta-potential. At the point of zero charge there is no net-charge. At low pH (<3) TiO_2 particles are likely to be protonated. The similarly charged particles therefore repel each other and agglomeration does not occur thus particle sizes will be small. At higher pH (>3) not all surface groups will be protonated and van der Waals forces between the O^- and OH_2^+ will cause agglomeration resulting in bigger particles.

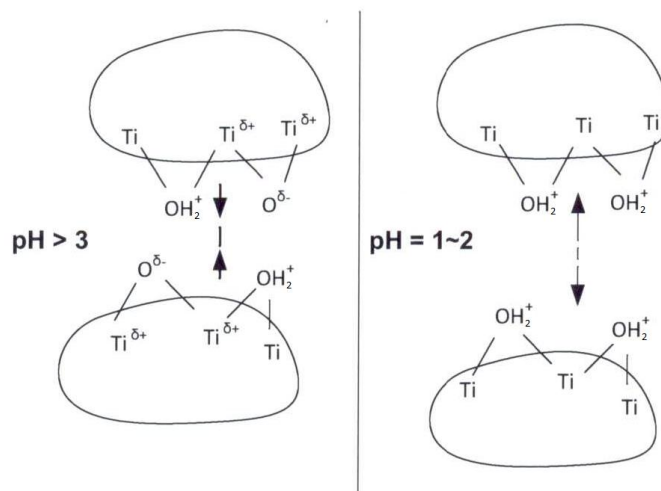


Figure 5. At high pH van der Waals forces attract particles, at low pH particles of similar charge repel each other. ^[20]

A colloidal suspension may also be stabilized by steric stabilization, the addition of certain polymers such as Polyvinyl Alcohol (PVA).^[21] Lyophobic parts of the polymer (trains) may adhere to lyophobic colloids while the lyophilic parts (tails) stick out in the dispersion medium. Steric stabilization works for charged as well as non-charged particles as it does not make use of the double-layer interaction between the colloids but of repulsive interaction between the lyophilic tails. Adhesion of the trains must be big enough to overcome the kinetic energy of a collision of particles.^[4]

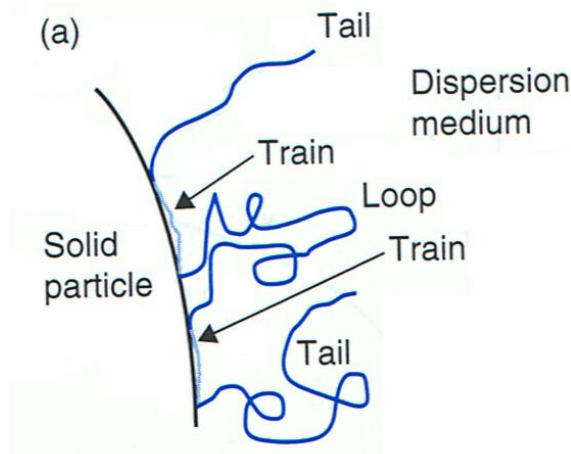


Figure 6. A polymer bound to a solid particle surface; Steric stabilization^[4]

In sintering of a coated colloidal suspension, it is this same effect that prevents grain growth and cracking of the surface. The stabilized films provide a better surface coverage and are more uniform than when not sterically stabilized.^[22] As a secondary effect in sintering, PVA creates porosity when the film is sintered above PVA's decomposition temperature, which is about 30-40 °C below its melting point (230 °C). Pore size increases for higher particle sizes and higher PVA concentration.^[21]

Smaller particles are more favorable for the TiO₂ immobilized catalyst as they have a larger surface area. Also, as the contact area between the catalyst and substrate is bigger for smaller particles, adhesion might be better than for larger particles. This would increase the mechanical stability of the TiO₂ film.^[20]

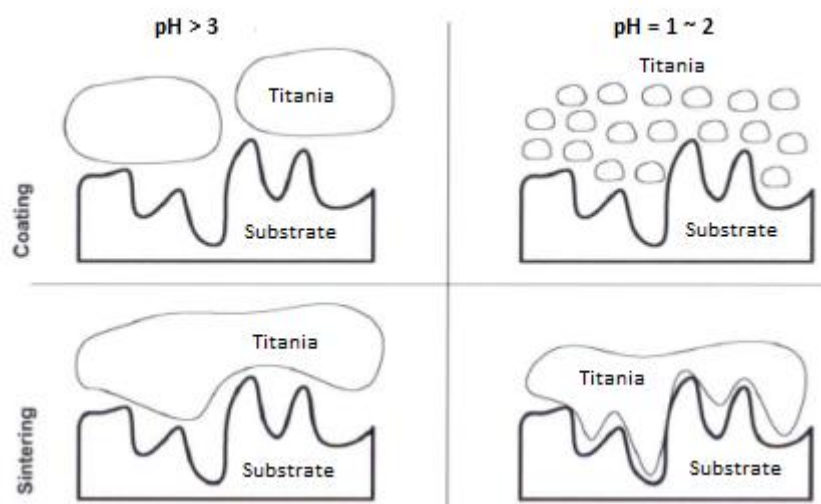


Figure 7. Influence of pH on the attachment of TiO₂ particles.^[20]

4.4 Microreactors

Microreactors have inner dimensions of less than a millimeter in size and therefore have many advantageous properties when used in photochemistry.^[1, 6, 10, 23] With their small dimensions they have a very high surface to volume ratio. They can show a specific surface area in the order of 10 000 m² m⁻³ to 50 000 m² m⁻³. This is much higher than conventional reactors that have specific surface areas in the order of 100 m² m⁻³ to 1000 m² m⁻³.^[24] As reaction rates strongly depend on the illuminated surface area of the photocatalyst, the high surface to volume area ratio is a very important property and may compensate for the loss of surface area resulting from the use of an immobilized catalyst.

The small characteristic length (L_c) of the smaller channels give microreactors a low Reynolds number (1-1000). The Reynolds number (Re) is the ratio of inertial forces (ρv) to viscous forces (μ/L_c) and indicates whether flow is laminar (Re < 2300) or turbulent (Re > 4000).

$$Re = \frac{\rho v L_c}{\mu} \quad (\text{Eq. 1.9})$$

With v = liquid average velocity, ρ = density of the liquid and μ = viscosity of the liquid. Microreactors therefore exhibit laminar flow.^[25]

In laminar flow the velocity profile is parabolic and mixing is limited to diffusion. In a macro-scale reactor diffusion rates are low because of low concentration gradients between the bulk and the catalyst surface. In microreactors however, the diffusion distance is much lower and this is accompanied by much higher gradients and diffusion rates enhancing mass-transport. In micro-scale mixers for example, mixing times can be shorter than a second while conventional stirrers can have mixing times up to several tens of seconds.^[24]

Another advantage of the shorter characteristic lengths is better light penetration. As the photocatalytic reaction relies on absorption of photons, an increase of light efficiency may increase the overall reaction efficiency.^[26]

Although not reported as much as conventional photocatalytic devices, microreactors have been shown to exhibit high conversion rates in photodegradation experiments. Matsushita et al. produced a microreactor out of Tempax plates which were bound by a self welding polymer in which a micro-channel was cut by laser ablation. One of the Tempax plates was coated with a TiO₂ layer using the sol-gel method.^[27] Other microreactors were made out of quartz or Pyrex with channels made by either micro-milling, wet etching process or laser ablation. The microreactors were shown to have a much higher activity than the conventional bulk reactors.^[10, 23, 28]

4.5 Analysis

4.5.1 UV spectroscopy

Absorption of light, the process that forms the basis of photocatalysis is also used for analytical purposes. UV spectrometers measure the amount of light absorbed by atoms and molecules at specific wavelengths. Upon absorption of light electrons are excited from the valence band to a higher energy state, the energy difference between the states corresponds to light in the UV-Vis region.^[3]

Absorbance (A) is related to the concentration of a sample by the Beer-Lambert law (Eq. 1.10) and is linear for dilute samples.

$$\log\left(\frac{I}{I_0}\right) = A = \epsilon \cdot l \cdot c \quad (\text{Eq. 1.10})$$

With I the transmitted intensity of light. I_0 the incident intensity of light. ϵ the molar extinction coefficient. And l the path length of the absorbing solution. Absorbance is usually measured at a wavelength corresponding to the max absorbance peak of the sample (λ_{max}). Both λ_{max} and ϵ are material properties but in a sample are affected by solvent.^[29]

4.5.2 Scanning Electron Microscopy

Conventional microscopes fail to image samples with structures on the nanometer scale because their resolution is limited to the wavelength of the light they use as a probe. For light microscopes this is in the micrometer range.^[29] Electron microscopy probes the sample with a beam of electrons instead of light. Scanning Electron Microscopy (SEM) detects secondary electrons, x-rays and backscattered electrons. Secondary electrons are generated when an incident electron is inelastically scattered and provide images of a very high resolution (up to 5-20 nm). Backscattered electrons are elastically scattered by the nuclei and are of higher energy than the secondary electrons. Samples of low atomic number give a low amount of backscattered electrons while the amount is higher for high atomic numbers. Backscattered electrons are therefore useful to image atoms by atomic contrast.^[3]

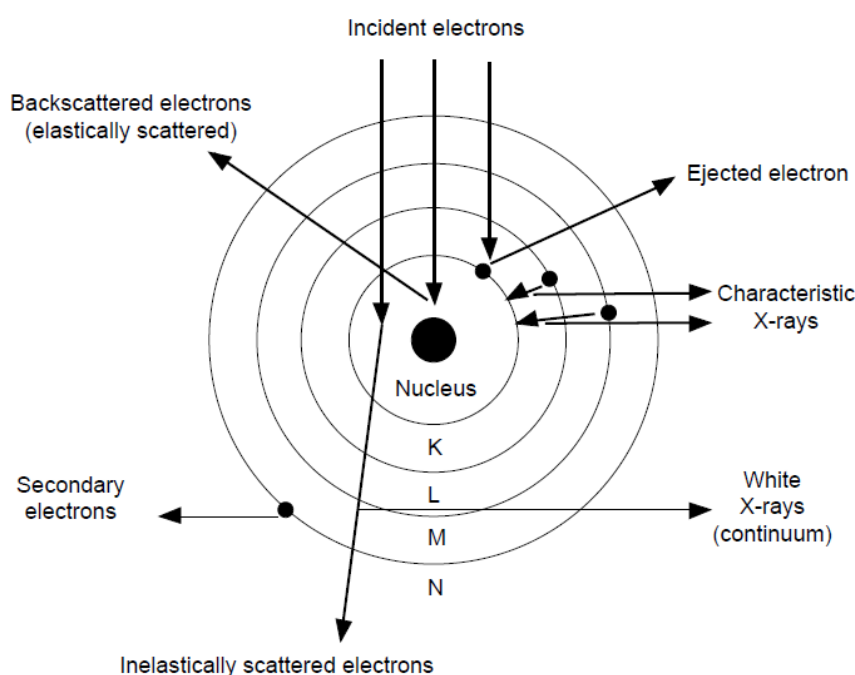


Figure 8. Backscattering, secondary electrons and X-rays in SEM^[3]

When a primary electron gives an inner shell electron sufficient energy to be ionized, an x-ray may be emitted when the excited inner shell electron falls back into its lower level. These x-rays are characteristic for the elements from which they have been formed and can be used to identify the atoms present.

SEM is conducted at low pressure as any present gas particles may cause unwanted scattering of the electrons. Furthermore, SEM is not suitable for non-conductible samples without treatment. A sputtered layer of a conductive material, such as gold, may enable imaging of such samples.

4.5.3 Tape testing

Tape testing is a quick and easy method to give an indication of the adhesion of a coated film. An adhesive tape is applied to the film surface and pulled off. The amount of coating removed is then subjectively rated to give a measure of the adhesion. Results of the tape test are affected by type of tape, pull-off velocity and angle. Shortcomings of the tape test are the subjectiveness and when the film sticks to the substrate it is difficult to distinguish between moderate, good or very good adhesion.^[2]

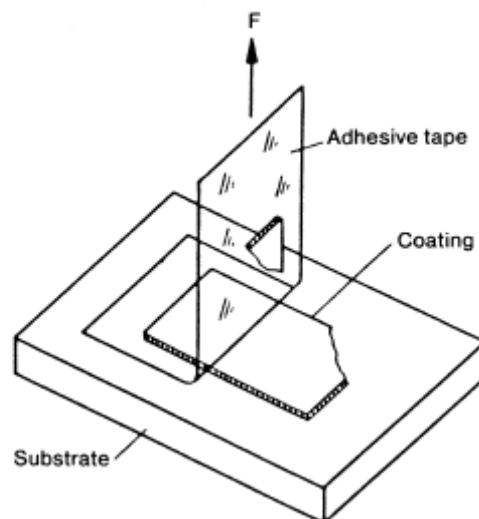


Figure 9. Depiction of the tape test. ^[2]

A less subjective variation on the regular tape test is the cross-cut test. A grid of squares is cut on the coated film after which the tape is applied and removed. The grid makes it easier to rate the amount of coating remaining using a scheme that distinguishes between 6 steps of results. (Figure 9)

The quantitative pull-off test uses a stud glued to the film and measures the amount of force needed to remove the stud. Requirement is that the adhesion of the glue to the film is stronger than the adhesion of the film to the substrate.

5 Experimental

Different recipes for immobilization of TiO_2 thin films have been applied to coat silicon substrates. The coated samples were tested and analyzed for surface quality and uniformity and mechanical stability. Using the most favorable recipes the microchannel was coated with TiO_2 and tested for its photocatalytic activity by degradation of methylene blue (MB) as the model compound.

5.1 TiO_2 immobilization

The TiO_2 immobilization procedure consists of 3 steps:

1) *Preparation of the suspension.* 1-3g TiO_2 powder (Aeroxide P25, 85% Anatase/15% Rutile, Evonik) and 1-10g Polyvinyl Alcohol (Mowiol 8-88, Aldrich Chemistry) was mixed with 50 ml 2-propanol (Merck) and 50 ml H_2O . After magnetically stirring for 3 hours the pH of the suspension was adjusted by adding acetic acid (Merck) to 2.8-6.6. PH was measured using a Metrohm AG 713 PH meter. The suspension with adjusted pH was left for magnetically stirring overnight at 50°C after which it was sonicated for 10-60 minutes.

2) *Coating of the substrate.* The silicon wafer (4 inch wafer, p type (100)) was manually cut into square chips after being cleaned in nitric acid (1hr; Merck) and rinsed with water and ethanol. Two different techniques were used to coat these chips: pipetting or spin coating. In both pipetting and spin coating the suspension was applied until the entire substrate was covered. In pipetting the substrate was then left to dry until most of the solvent evaporated. In spin coating the chip was then spin coated for 50 seconds at 500-2000 RPM, leaving a thin layer on the substrate.

3) *Sintering.* To sinter the TiO_2 film and remove all remaining solvent and PVA the coated substrate was put in a high temperature oven ($400\text{-}600^\circ\text{C}$). Heating was done in three steps: heating the oven to the desired temperature in 230 minutes, keeping it at the desired temperature for 120 minutes and cooling down the oven in 230 minutes.

In order to test the influence of the substrate on TiO_2 adhesion, in a special case a thin layer of gold was electron sputtered on the silicon substrate before coating with TiO_2 . A sputterer (Balzers Union SCD 040) was used at 13 mA current and 200-220 W. The sputtering duration was 3 minutes for a thin layer and 10 minutes for a thicker layer.

Recipe	Deposition Method	P25	PVA	pH	Sonicated	Sintering T	Analysis
1A	Pipetting	1g	1g	3.4	12 min	500 °C	SEM Imaging, Tape tested
1B	Pipetting	1g	0g	2.8	12 min	500 °C	SEM Imaging, Tape tested
1C	Pipetting	1g	1g	2.8	12 min	500 °C	SEM Imaging, Tape tested
2A	Spin coating (500-2000 RPM)	1g	5g	2.8	60 min	400-600 °C	SEM Imaging, Tape tested
2B	Spin coating (2000 RPM)	1g	10g	2.8	60 min	500 °C	SEM Imaging, Tape tested, Photocatalytic Activity, Thickness
2C	Spin coating (2000 RPM)	3g	5g	2.8	60 min	500 °C	SEM Imaging, Tape tested
2D	Spin coating (500-2000 RPM)	1g	5g	2.8	60 min	400-600 °C	SEM Imaging, Tape tested, Photocatalytic Activity, Thickness
2E	Spin coating (2000 RPM)	1g	5g	3.8	60 min	500 °C	SEM Imaging, Tape tested
2F	Spin coating (2000 RPM)	1g	5g	6.6	60 min	500 °C	SEM Imaging, Tape tested
2G	Spin coating (2000 RPM)	1g	5g	4.5	60 min	500 °C	SEM Imaging, Tape tested
2H	Spin coating (On sputtered Gold)	1g	5g	2.8	60 min	500 °C	SEM Imaging, Tape tested

Table 2. TiO_2 coating recipes, 50ml H_2O and 50ml 2-propanol added.

5.2 Fabrication of the microreactor



Figure 11. Depiction of the microreactor

A silicon substrate coated with TiO_2 and a Polydimethylsiloxane (PDMS) chip containing the microchannels on top were bound to create the microreactor. On a silicon wafer, two different channel configurations were made using photolithography by negative photo resist (SU-8). Initially SU-8 was spun at 500 rpm for 10 seconds and continued to 1000 rpm for 30 seconds. Then the sample was prebaked at 50° , 65° , 95° for 10, 10, 45 minutes respectively. This was followed by UV-exposure for 33 seconds and post baking at 50° , 65° , 80° for 5, 10, 20 minutes respectively. Finally the sample was spray developed by RER 600 as the developer. The resulted SU-8 height was 100-150 μm as revealed by surface profiler which corresponds to channel depth after PDMS casting.

To prepare the PDMS, polymer base (RTV-615 A, Permacol bv) and curing agent (RTV-615 B, Permacol bv) were mixed in a 10:1 ratio as advised by the manufacturer. After mixing and degassing in a desiccator the PDMS was cast on the patterned wafer in a petri dish. After degassing for the second time the PDMS was left to cure at 60°C for 2 hours.

After crosslinking the PDMS was released from the patterned wafer and cut in chips. These chips were bound to a square TiO_2 coated silicon substrate by three different methods: plasma oxidation, using an optical adhesive (Norland optical adhesive 78 or 91) or only partially curing the PDMS before bringing it in contact with the coated substrate. Before binding, the PDMS was pierced using a needle with an inner diameter of 0.61 mm and outer diameter of 0.91 mm to create an inlet and outlet.

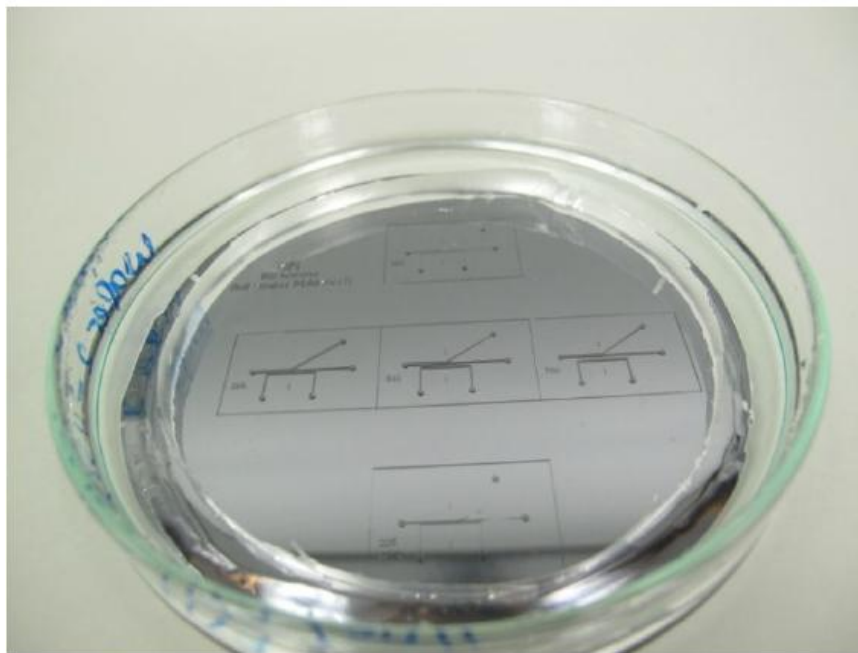


Figure 12. Wafer in petri dish after releasing PDMS. [30]

To bind by plasma oxidation a Plasma Fab 508 was used. The coated silicon substrate and PDMS chip were placed in the middle of the plasma oxidation chamber, inner surface pointing up. Power and duration of exposure was varied between 50-200 W and 0.5-10 minutes respectively, optimizing the adhesion. As reference the procedure was also applied to an uncoated silicon substrate.

The optical adhesive was applied to a roller and gently rolled onto the PDMS surface, preventing any of the glue to enter the channels. The PDMS was then brought in contact with the coated substrate and a small amount of pressure was applied before curing the glue under UV radiation.

In only partially the curing the PDMS before bringing it in contact with the coated substrate, the PDMS chips were peeled off after curing 45-50 minutes at 60 °C instead of after 2 hours. In this condition the PDMS takes its shape but still is sticky. After bringing the PDMS in contact with the coated substrate, it was left to cure in the 60 °C oven for another hour to complete the curing process.

The method showing best adhesion and lowest rate of failure was afterwards used to create the microreactors for photocatalytic performance assessment.

The channels are shown in figure 13. In the experiments only the bottom channel was used. Dimensions are 250 μm (Width) x 150 μm (Depth), length of 18 mm and a volume of 0.675 μL .

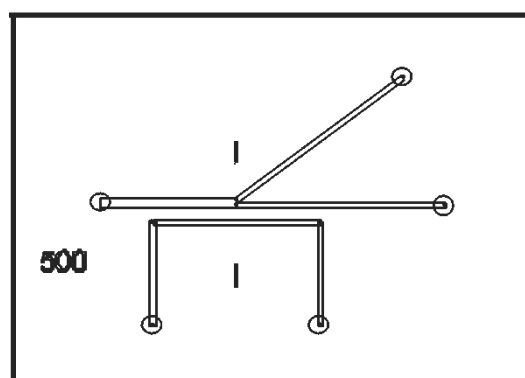


Figure 13. Chip design ^[30]

5.3 Analysis

5.3.1 Scanning Electron Microscope

Surface uniformity was evaluated using a Scanning Electron Microscope (JSM-5006LV). Pictures were made in surface and cross sectional view.

5.3.2 Tape testing

Mechanical stability was qualitatively determined by tape testing using scotch tape. Tape was applied on the surface and removed at a consistent angle and speed. Surface uniformity before tape testing, amount of coating remaining after tape testing and amount of coating visible on the tape were rated on a scale of 1-10.

5.3.3 Photocatalytic activity

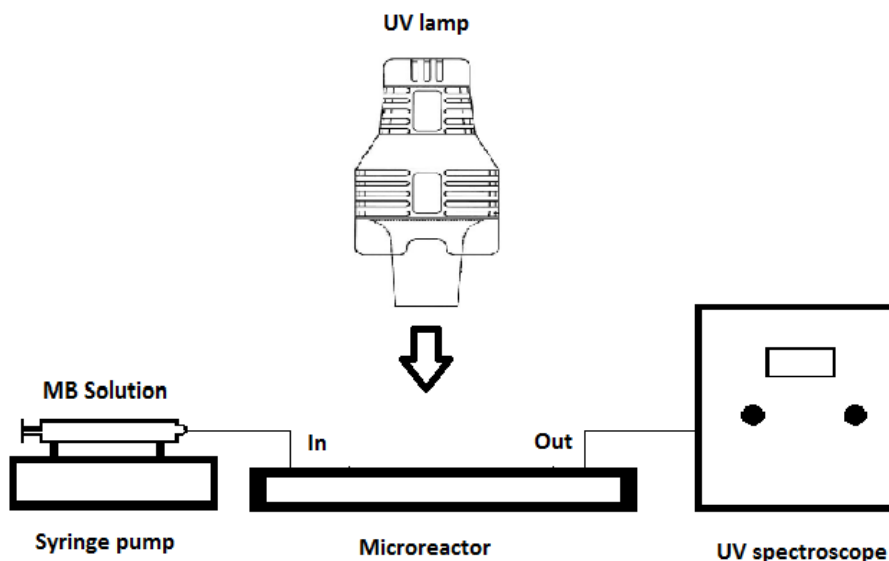


Figure 14. Experimental setup for MB degradation.

The activity of the catalyst was tested by degradation of methylene blue (MB; Fluka Analytical). The experimental setup in figure 14 was used to flow a 0.08 mM solution of MB through the microreactor. A syringe pump was used at flowrates of 1,3,5,7 and 10 $\mu\text{l}/\text{min}$. The absorbance of the outlet yield was measured by an UV spectrometer (Varian UV-Vis detector model 34c) set to 664 nm which corresponds to the MB absorbance peak (figure 15). Absorbance was converted to MB concentration using a calibration plot.

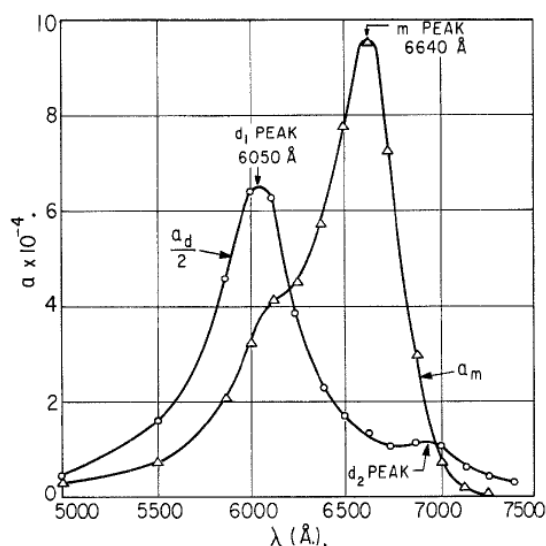


Figure 15. Molar absorbance indices of pure monomer (a_m) and dimer (a_d) of aqueous methylene blue solutions.^[31] Max absorbance peak corresponds to a wavelength of 664 nm.

Turning on the flow, MB is absorbed on the catalyst surface giving inaccurate absorbance readings. Therefore flow was allowed to reach steady state before illuminating the microreactor with the UV light. Turning on the UV light initiated the photocatalytic reaction and outlet absorbance was measured until a new steady state was achieved. With a calibration plot absorbance was converted to concentration and the total degradation was calculated.

6 Results and Discussion

All TiO₂ coating recipes described in the experimental section were used to coat flat silicon substrates. All recipes were analyzed by SEM and the mechanical stability of most samples was tested by tape testing. The most successful coating recipes were applied in a microreactor in the MB degradation experiments. An overview of all coated and used samples is shown in Appendix A; an overview of SEM images per coating recipe is shown in Appendix B.

6.1 Immobilization

The first series of samples was coated to find a stable and suitable TiO₂ immobilization-method that could be applied in the photocatalytic microreactor. Different TiO₂ coatings which were prepared by various recipes and different parameters were deposited by pipetting and spin coating on roughly 10 by 10 mm silicon chips. Subsequently their uniformity and mechanical stability were evaluated. Tape testing results are shown in figure 16.

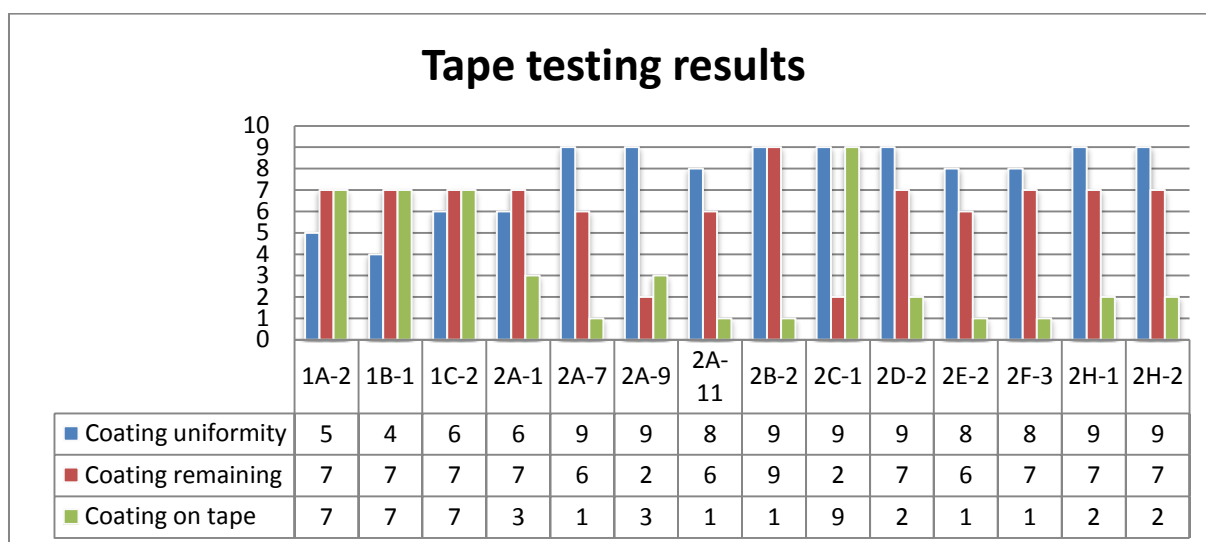


Figure 16. Tape testing results. Rated on a scale of 1-10.

6.1.1 Pipetted samples

Surface uniformity varied per recipe. Samples coated by pipetting showed a lower surface uniformity than samples coated by spin coating. All pipetted samples showed a coffee stain effect, caused by slow evaporation of the solvent. Recipe 1A was similar to the recipe used by Aran et al.^[11] but did not result in a uniform and stable layer. A buildup of coating in the middle of the substrate detached after sintering. Lowering the pH of the suspension (1C) resulted in the same buildup of coating as in recipe 1A. The buildup did not detach after sintering, but 1C was not given higher tape testing scores than 1A as the buildup did detach after the tape was removed. SEM imaging showed that in the areas where no buildup had occurred the film was uniform. However, large crystal-like contaminants were visible on the SEM images of 1C.

In recipe 1B where no PVA was used, many small cracks were observed after sintering. The cracks are clearly visible in the SEM micrograph (figure 17). PVA limits grain growth by steric stabilization and providing a structure to the coating. Without the polymeric binder, grain growth occurred freely during the sintering process which results in a cracked surface.^[22]

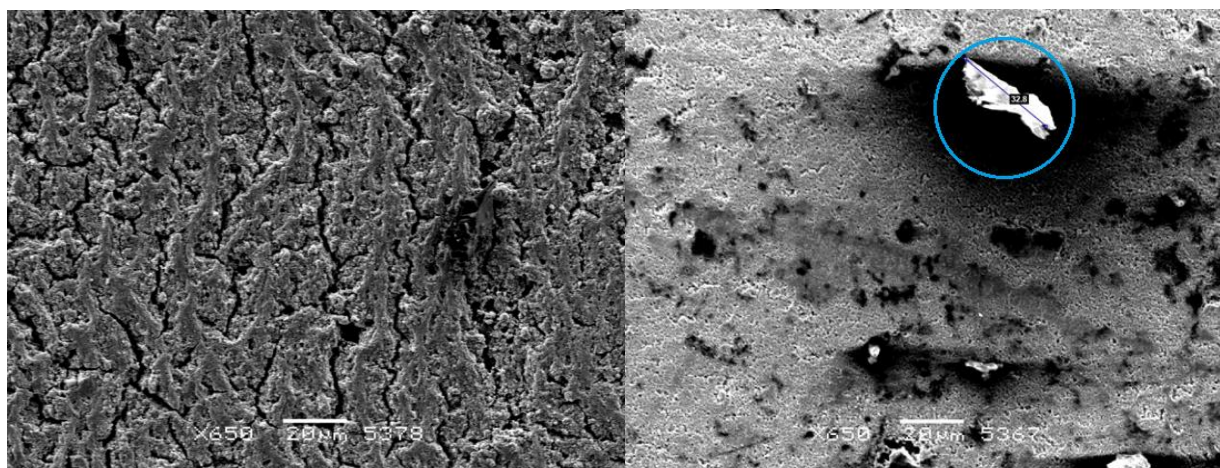


Figure 17. (Left) SEM image of 1B-2 showing the cracked surface; (Right) SEM image of 1C-1. Surface is moderately uniform but contaminations are present.

All pipetted recipes had a moderate amount of coating remaining after tape testing, but the high amount of coating visible on the tape indicates that the adhesion of the pipetted films is not optimum.

6.1.2 Spin coated samples

Spin coating requires a more viscous suspension. Therefore instead of 1g PVA (1A), 5g PVA was used at pH 2.8 (2A). Samples coated at 500-1000 RPM for 50 seconds were moderately uniform, but the highest uniformity and substrate coverage were achieved at 2000 RPM for 50 seconds. On all other spin coated samples those settings were used.

The flake-like contaminants observed in recipe 1C were also seen in samples 2A, 2B and 2C. On the suspension 2D, instead of mixing the P25, PVA and solvent at the same time, at first only the P25, water and 2-propanol were added together. After magnetically stirring for 1 hour the PVA was added and the suspension was left to stir magnetically another 2 hours. As a result the contaminants were not observed as shown in figure 18. The new mixing order was used on all coated samples after 2D (2D-2H).

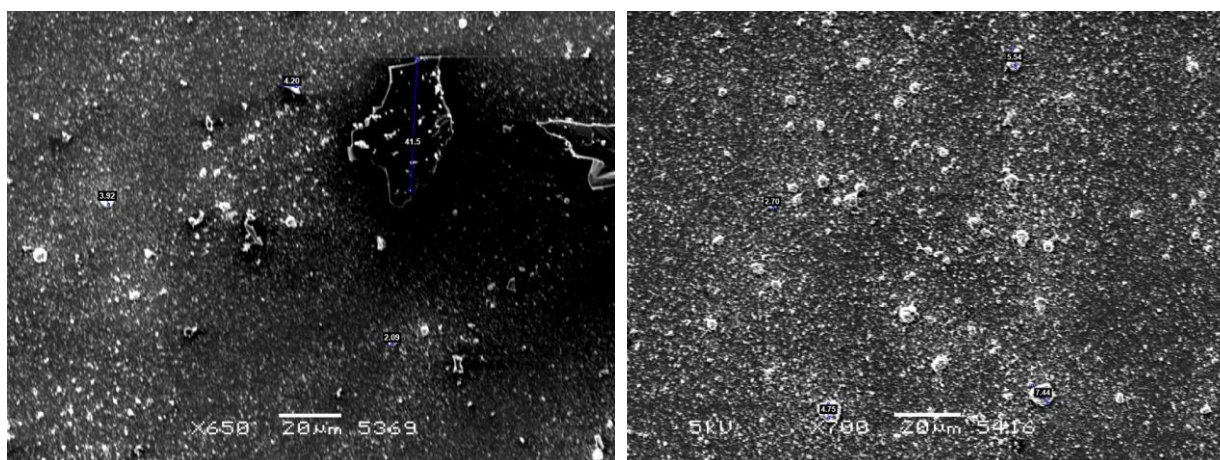


Figure 18. SEM images of 2A-5 (Left) and 2D-1 (Right).

Sintering temperature of the samples coated by recipe 2A was set to 400, 500 or 600 °C. All samples were very uniform on sight but tape testing results varied. Samples 11 and 7, sintered at 500 °C and 600 °C respectively, showed an amount of coating remaining on the substrate similar to the pipetted samples after tape testing. However, amount of coating visible on the tape was much lower, indicating a better adhesion to the substrate. Sample 9, sintered at 400 °C, didn't show such a good mechanical stability: tape testing removed almost the entire film. Mechanical stability appears to increase at higher sintering temperatures.

Moreover the effect of the sintering temperature on the TiO₂ agglomerations was investigated. By increasing the sintering temperature, the number and size of agglomerations increased. In turn, the presence of more agglomerations had adverse effect on the robustness of the coating as revealed by tape testing.

In recipe 2B where 10g PVA was used, the mechanical stability enhanced noticeably. This was proven by presence of high amounts of coating after tape testing. (figure 19)

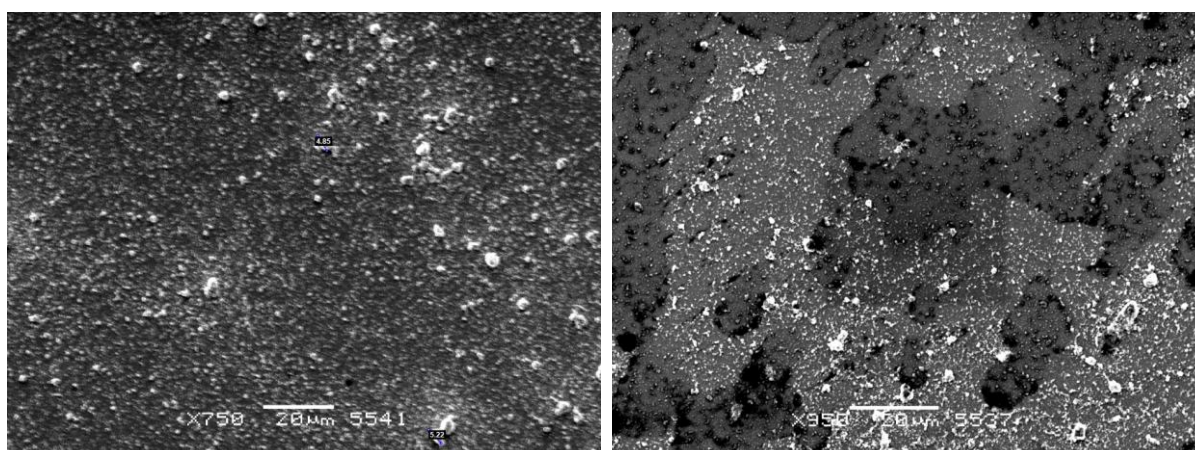


Figure 19. SEM image of sample 2B-2 (Left) before tape testing and SEM image of sample 2B-3 (Right) after tape testing. A high amount of coating remained.

Increasing the P25 concentration (2C) resulted in contaminations, bigger agglomerations and after tape testing almost the entire film was removed.

Recipes 2E, F and G had a variation in pH of the suspension: 3.8, 6.6 and 4.5 respectively. An increase in agglomeration size was expected as PH increased. On the SEM images the bigger agglomerations at higher PH were visible, but mechanical stability was comparable to the suspensions at lower pH. The effect of smaller particles on adhesion and mechanical stability as described in section 3.3 was not shown.

The samples with a sputtered layer of gold (2H) had better quality SEM images but uniformity and mechanical stability was comparable to samples coated with the same recipe on silicon substrates without the sputtering treatment (2D).

Recipes 2D and 2B were concluded to be the most stable and potentially most photocatalytically active recipes and were tested for their photocatalytic activity in the MB degradation experiments.

6.2 Microreactor fabrication

Following the preparation of the first series of prepared samples, the most optimum TiO₂ coatings were used in the PDMS based photocatalytic microreactor. Employing recipe 2D sintered at 400 °C, 500 °C and 600 °C and using recipe 2B sintered at 500 °C the microreactor was fabricated as described in the experimental section and used in the MB degradation experiments. To make sure to eliminate the effect of UV-light itself on the degradation of MB, one microreactor was fabricated without TiO₂ coating.

Binding the PDMS to the coated substrate by plasma oxidation was unsuccessful. Multiple exposure times and plasma power settings were tried as described in the experimental section. At an exposure time of 30 seconds at 100W, the PDMS attached to an uncoated substrate without leakage. The PDMS and substrate were unable to be separated without damaging the PDMS. When the same or other settings were used on the coated substrate, there was no adhesion of the PDMS at all. The Si-O-Si bonds that caused the strong adhesion of the uncoated substrate were shielded by the TiO₂ film.

The use of both Norland optical adhesive 78 and 91 resulted in a reasonable binding of the PDMS and substrate, but leaking occurred during the photodegradation experiments.

The third binding method, bringing the PDMS in contact with the substrate after only partially curing it, proved to be the best approach. Using this method, microreactors adequate to be used in the MB degradation experiments were created. However, failure rate on binding was still high, 1 out of 3 attempts showed leakage. A thicker layer of PDMS (≈ 7 mm) with a longer curing time before bringing it in contact with the substrate (>50 minutes) was more rigid and more likely to show leakage. A thinner layer of PDMS (≈ 4 mm) with a shorter curing time before bringing it in contact with the substrate (<45 minutes) was very sticky but fragile and could tear when peeled of the wafer or when inlet and outlet were punctured. A PDMS layer of about 4 mm thickness and a first phase curing time between 45 and 50 minutes, varying per sample, resulted in the lowest failure rate.

6.3 Photocatalytic activity

6.3.1 Calibration

Running solutions of different MB concentration through the UV-spectroscope a calibration plot was made. MB concentration varied between 0.01 and 0.1 mM. The calibration plot was taken in a region linear according to the beer-lambert law and was used to convert the absorbance of the yield in the photodegradation experiments to MB concentration. Concentration was related to absorbance by:

$$C = \frac{A - 0,0052}{0,6422} \quad (\text{Eq. 5.1})$$

With C the outlet concentration, and A the measured absorbance at 664 nm.

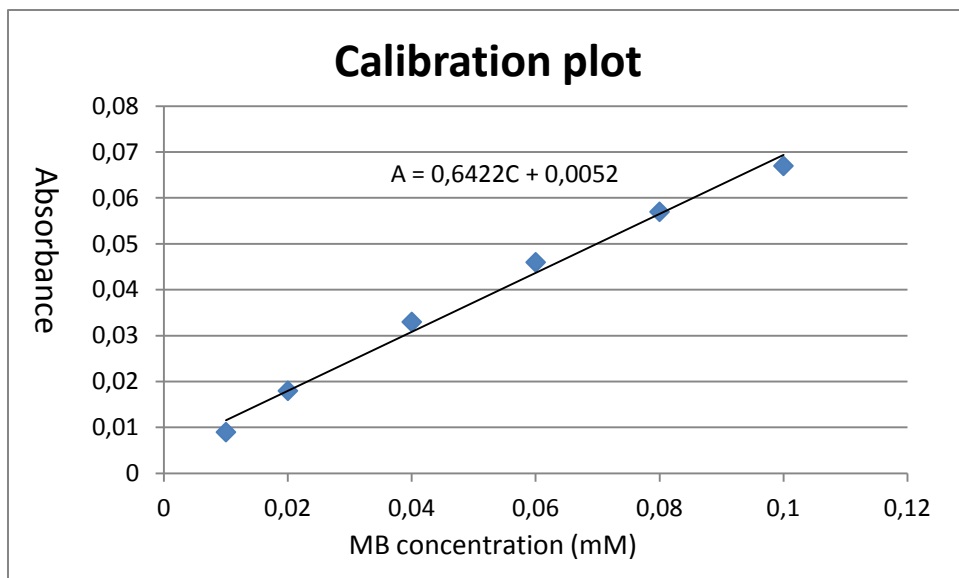


Figure 20. MB calibration plot. Used to convert measured Absorbance to concentration.

6.3.2 Methylene Blue degradation

Degradation efficiency of the microreactors was determined by measuring the MB concentration after passing through the microreactor at the different flowrates as described in the experimental section. Data points were manually taken every 5 minutes.

Absorption of MB on the catalyst surface settled after approximately 35-45 minutes at 10 $\mu\text{l}/\text{min}$ and 100-120 minutes at 1 $\mu\text{l}/\text{min}$. The UV light was not turned on until steady state was achieved, defined as three constant measurements at higher flowrates and 5 constant measurements at lower flowrates. Once the UV-light was turned on, absorbance would decrease, indicating the degradation of MB. Once a new steady state was achieved the UV-light was turned off. Flow was continued and adjusted to the next flowrate as soon as the MB concentration was back to 0.08 mMol and the process was repeated.

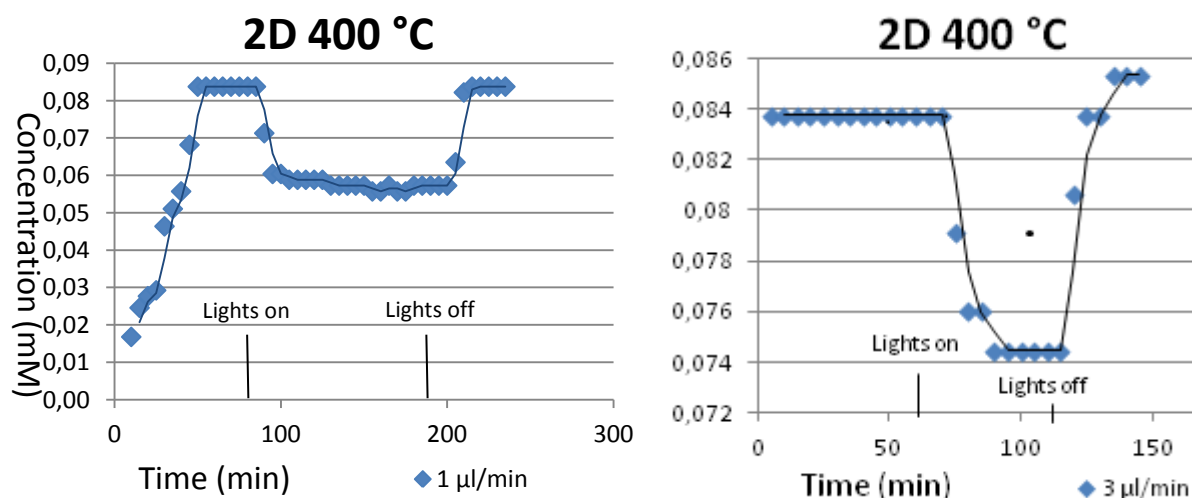


Figure 21. Methylene Blue degradation measurements of 2D 400 °C at 1 $\mu\text{l}/\text{min}$ (left) followed by 3 $\mu\text{l}/\text{min}$ (right).

Concentration was converted to degradation by:

$$Degradation = \frac{C_{in} - C_{out}}{C_{in}} \cdot 100\% \quad (\text{Eq. 5.2})$$

With C_{in} the outlet concentration of MB without UV illumination and C_{out} the lowest outlet concentration measured during UV illumination. Results of all microreactors are shown in figure 22.

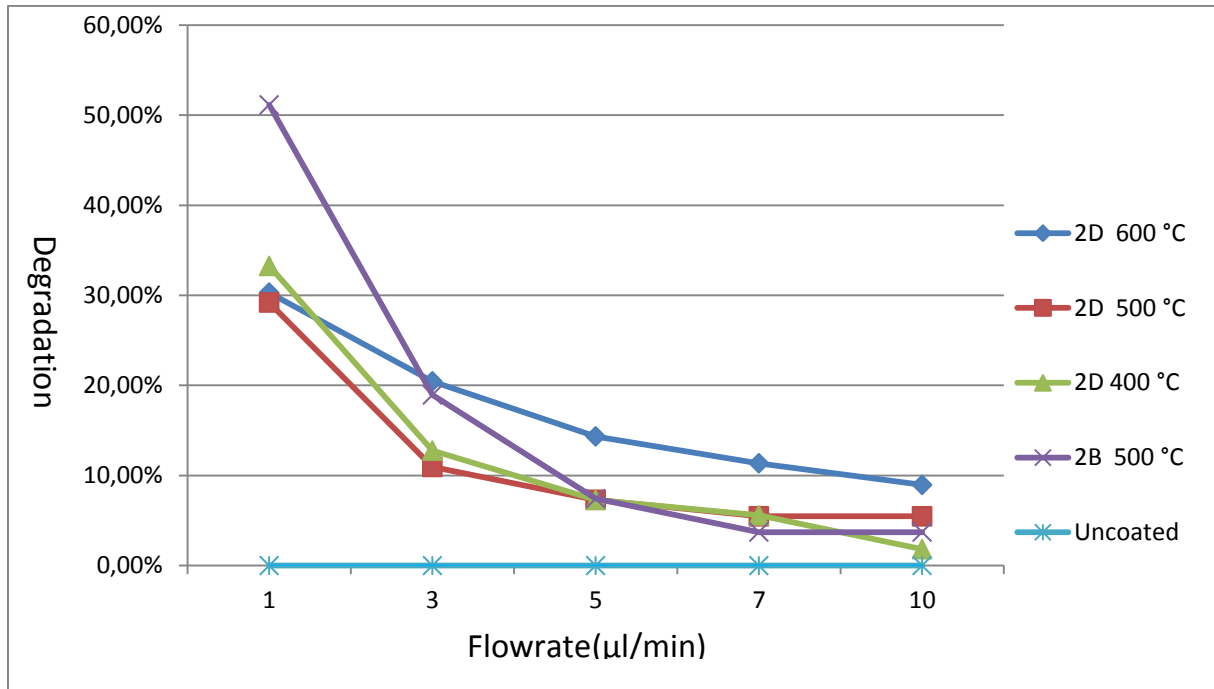


Figure 22. MB degradation of the different microreactors at different flowspeeds.

The uncoated microreactor did not show any photocatalytic activity indicating that the degradation effect on the coated samples is due to the presence of the TiO_2 film. At the lowest flowrate (1 $\mu\text{l}/\text{min}$), recipe 2B 500 °C had the highest activity with a degradation of 51.14%, followed by 2D sintered at 400 °C (33.26%), 600 °C (30.30%), and 500 °C (29.20%) respectively. At higher flowspeeds total degradation was lower for all samples as the residence time was shorter. At the highest flowrate (10 $\mu\text{l}/\text{min}$) 2D sintered at 600 °C had the highest activity (8.96%) and 2B 500 °C and 2D 400 °C had the lowest activity (3.72% and 1.82% respectively).

Such conflicting results were not expected, but could be explained by an inconsistency in the experiments. The measurements on the first two microreactors (2D 600 °C and 2D 500 °C) were done in order of highest to lowest flowrate while on the others (2D 400 °C and 2B 500 °C) measurements were done in order of lowest to highest flowrate. Catalyst inactivation or erosion due to shear is likely to occur after operation. This would mean that 2D 600 °C and 2D 500 °C had a fresher catalyst surface at the higher flowrates, and 2D 400 °C and 2B 500 °C at the lower flowrates.

Another inconsistency could be caused by failed binding attempts and experiments that were redone. Some microreactors had been operated for a longer time than others before the measurements were successful. This was more apparent on the first two microreactors as the procedure was still being optimized.

7 Conclusions and recommendations

The aim of this study was to evaluate different recipes for immobilization of TiO_2 on silicon substrates and to find a suitable recipe to be applied in a microreactor. In this work thin films of TiO_2 were made by pipetting or spin coating a colloidal suspension of Previously Made Titania Powder (PMTP) on silicon substrates. Influence of sintering temperature, steric stabilization and pH of the suspension, P25 concentration and spin coating settings on the morphology and mechanical stability of the film were investigated by Scanning Electron Microscopy (SEM) and tape testing. The most favorable recipes were applied in a photocatalytic microreactor which was made by binding a PDMS chip containing a microchannel to a coated silicon substrate. The microreactor was used for analysis of the film's photocatalytic activity by degradation of methylene blue.

7.1 General conclusions

Spin coating was found to be a more effective coating technique than pipetting. Spin coating was effective in evenly spreading the colloidal suspension and evaporating the solvent leading to a uniform surface and a well-covered substrate. The low evaporation rate of the solvent in pipetting allowed for capillary flow and caused buildups of TiO_2 particles. Pipetting did not lead to a uniform surface or a well-covered substrate. Mechanical stability of spin coated samples was higher than of the pipetted ones, however this might also be dedicated to the higher amount of PVA used in the spin coated recipes.

Stabilizing the colloidal suspension was an important part of the coating procedure. With addition of PVA as a steric stabilizer and acetic acid to lower pH lower amount of agglomeration was observed in SEM images. Addition of PVA also increased mechanical stability by providing a structure to the coating before sintering. Without PVA sintering would result in a cracked surface.

Sintering increased the mechanical stability of the film, but no improvement was observed at temperatures higher than 500 °. Although higher sintering temperatures result in stronger films, it also leads to grain growth, anatase to rutile conversion and agglomeration because of higher diffusion rates. Larger particle sizes, collapse of pores and structure caused by grain growth and the conversion to rutile should lead to a lower surface area and thus a lower activity of the catalyst. The effect of sintering and PVA on photocatalytic activity was analyzed by degradation of MB in a microreactor.

Increasing P25 concentration lead to a decrease in mechanical stability. Sputtering a thin layer of gold on the silicon substrates before coating with TiO_2 did not improve film quality.

Applying the coating procedure in a microreactor proved challenging. Binding the PDMS chips to the coated substrates by plasma oxidation or an optical adhesive failed. By bringing the PDMS in contact with the coated substrate after only partially curing, a successful binding method was found. Problems arose from the porous TiO_2 film that shielded Si-O-Si bonds in plasma oxidation or caused leaking when the optical adhesive was used. Alternative methods such as binding the chip before coating by flushing the TiO_2 suspension through a closed channel might have given problems with light penetration as all sides of the channel would be covered by TiO_2 .

The successfully fabricated microreactors were used to test the photocatalytic activity of recipes 2D at 400 °C, 500 °C and 600 °C and 2B at 500 °C. The photocatalytic effect of the TiO₂ film was shown: even for a small reactor volume a high activity was achieved. However due to inconsistent results no conclusions can be drawn on the effect of sintering temperature and amount of PVA on the activity of the film.

7.2 Recommendations

A lot of experimental work has been done to evaluate the immobilization procedure of TiO₂ films. However, a lot of film characteristics such as porosity, crystal structure, surface area and film thickness are yet to be investigated or deserve more attention. Further investigation of these characteristics can help to understand why some coating recipes result in a more stable and more active film than others. It is also recommended to make a theoretical model of the microreactor and to confirm the experimental results.

The application of the coating in a microreactor was successful and although no conclusions could yet be drawn on the influence of certain parameters on the photocatalytic activity of the films, a good start has been made. It is recommended to repeat the MB degradation experiments to find the influence of sintering temperature, amount of steric binder and other parameters. While repeating the experiments it is important to make sure each sample has seen the same amount of operating hours and order of measurements is kept consistent.

As failure rate of binding by partially curing was still high it is also recommended to explore other binding methods. Binding of PDMS to silicon is well documented and focus should be in finding a way to prevent the TiO₂ film from interfering in the binding process. Theoretical modeling of light penetration through the TiO₂ film or silicon substrate might be useful to find out whether light still reaches the catalyst surface when all reactor walls are coated or when the microreactor is lighted from the back. This would make it possible to coat the microreactor by flushing the TiO₂ suspension through the channels after binding.

8 References

1. Fujishima, A., X. Zhang, and D. Tryk, *TiO₂ photocatalysis and related surface phenomena*. Surface Science Reports, 2008. **63**(12): p. 515-582.
2. Dr. A. Bergauer, D.C.E.-S., *Lecture notes - Physics and Technology of Thin Films*1993: TU Wien.
3. Faust, B., *Modern Chemical Techniques*1997: Royal Society of Chemistry.
4. I.R.Gentle, G.T.B., *Interfacial Science: an introduction* 2nd ed2010, New York: Oxford University Press.
5. Carp, O., C.L. Huisman, and A. Reller, *Photoinduced reactivity of titanium dioxide*. Progress in Solid State Chemistry, 2004. **32**(1-2): p. 33-177.
6. Van Gerven, T., et al., *A review of intensification of photocatalytic processes*. Chemical Engineering and Processing, 2007. **46**(9): p. 781-789.
7. Lindstrom, H., R. Wootton, and A. Iles, *High surface area titania photocatalytic microfluidic reactors*. Aiche Journal, 2007. **53**(3): p. 695-702.
8. Shan, A.Y., T.I.M. Ghazi, and S.A. Rashid, *Immobilisation of titanium dioxide onto supporting materials in heterogeneous photocatalysis: A review*. Applied Catalysis a-General, 2010. **389**(1-2): p. 1-8.
9. Doll, T.E. and F.H. Frimmel, *Development of easy and reproducible immobilization techniques using TiO₂ for photocatalytic degradation of aquatic pollutants*. Acta Hydrochimica Et Hydrobiologica, 2004. **32**(3): p. 201-213.
10. Matsushita, Y., et al., *Photocatalytic reactions in microreactors*. Chemical Engineering Journal, 2008. **135**: p. S303-S308.
11. Aran, H.C., et al., *Porous Photocatalytic Membrane Microreactor (P2M2): A new reactor concept for photochemistry*. Journal of Photochemistry and Photobiology a-Chemistry, 2011. **225**(1): p. 36-41.
12. Hoffmann, M.R., et al., *Environmental Applications of Semiconductor Photocatalysis*. Chemical Reviews, 1995. **95**(1): p. 69-96.
13. Saupe, G.B., et al., *Evaluation of a new porous titanium-niobium mixed oxide for photocatalytic water decontamination*. Microchemical Journal, 2005. **81**(1): p. 156-162.
14. Villarreal, T.L., et al., *Semiconductor photooxidation of pollutants dissolved in water: A kinetic model for distinguishing between direct and indirect interfacial hole transfer. I. Photoelectrochemical experiments with polycrystalline anatase electrodes under current doubling and absence of recombination*. Journal of Physical Chemistry B, 2004. **108**(39): p. 15172-15181.
15. Hamasaki, Y., et al., *Photoelectrochemical Properties of Anatase and Rutile Films Prepared by the Sol-Gel Method*. Journal of the Electrochemical Society, 1994. **141**(3): p. 660-663.
16. Silva, C.G. and J.L. Faria, *Effect of key operational parameters on the photocatalytic oxidation of phenol by nanocrystalline sol-gel TiO₂ under UV irradiation*. Journal of Molecular Catalysis a-Chemical, 2009. **305**(1-2): p. 147-154.
17. Zhao, Y., et al., *Enhanced photocatalytic activity of hierarchically micro-/nano-porous TiO₂ films*. Applied Catalysis B-Environmental, 2008. **83**(1-2): p. 24-29.
18. Liu, Y., et al., *Sonochemical synthesis and photocatalytic activity of meso- and macro-porous TiO₂ for oxidation of toluene*. Journal of Hazardous Materials, 2008. **150**(1): p. 153-157.
19. Yanhui Ao, J.X., Degang Fu, Chunwei Yuan, *Preparation of porous titania thin film and its photocatalytic activity*. Applied Surface Science, 2008. **255**: p. 3137-3140.
20. Rijnaarts, T., *Porous Photocatalytic Membrane Microreactors (P2M2): novel reactor design*, in *Soft matter, Fluidics & Interfaces*2010, University of Twente: Enschede.
21. Mikkola, P., et al., *Colloidal processing of aluminum oxide powder for membrane applications*. Ceramics International, 2003. **29**(4): p. 393-401.
22. Garzella, C., et al., *TiO₂ thin films by a novel sol-gel processing for gas sensor applications*. Sensors and Actuators B-Chemical, 2000. **68**(1-3): p. 189-196.
23. Matsushita, Y., et al., *Photocatalytic N-alkylation of benzylamine in microreactors*. Catalysis Communications, 2007. **8**(12): p. 2194-2197.
24. Jahnisch, K., et al., *Chemistry in microstructured reactors*. Angewandte Chemie-International Edition, 2004. **43**(4): p. 406-446.
25. McCabe, W.L., J.C. Smith, and P. Harriott, *Unit operations of chemical engineering (6th edition)*2001, New York: McGraw-Hill.
26. Gorges, R., S. Meyer, and G. Kreisel, *Photocatalysis in microreactors*. Journal of Photochemistry and Photobiology a-Chemistry, 2004. **167**(2-3): p. 95-99.
27. Matsushita, Y., et al., *N-alkylation of amines by photocatalytic reaction in a microreaction system*. Catalysis Today, 2008. **132**(1-4): p. 153-158.
28. Matsushita, Y., et al., *Recent progress on photoreactions in microreactors*. Pure and Applied Chemistry, 2007. **79**(11): p. 1959-1968.
29. Peter Atkins, J.d.P., *Atkins' Physical Chemistry*. 8 ed2006: Oxford University Press.
30. Ijmker, H.M., *Desalination by Ion Concentration Polarization*, in *Soft Matter, Fluidics and Interfaces*2011, University of Twente.
31. Bergmann, K. and C.T. Okonski, *A SPECTROSCOPIC STUDY OF METHYLENE BLUE MONOMER, DIMER, AND COMPLEXES WITH MONTMORILLONITE*. Journal of Physical Chemistry, 1963. **67**(10): p. 2169-&.

9 Acknowledgements

It has been a few months since I started my bachelor assignment as a completion to my degree in Advanced Technology. It was thanks to Pim Bullée, who aroused my interest with his own bachelor assignment, that I was pointed towards the SFI group where I was given this assignment by Rob Lammertink. The very practical assignment of evaluating TiO₂ coating procedures sounded interesting as it would require working with a lot of lab-equipment, providing me with a good opportunity to obtain more experience in working in a laboratory. I enjoyed my stay at the SFI group and looking back at the process, I think I can be satisfied with the results.

First of all I would like to thank my direct supervisor Damon Rafieian for his guidance throughout my research. We have shared a lot of time working together in the lab, measuring, discussing, finding solutions to (un)expected problems and working with equipment both of us had not worked with before. Damon, I hope my results can be of good use to you and wish you good luck in finishing your PhD.

I would like to thank Rob Lammertink for his suggestions and help during our weekly meetings. You have been a great source of information and could always point me in new directions when I did not know where to go with my research.

Also, much gratitude goes out to: Can Aran for being a great help with the experimental setup for the photocatalytic degradation of MB, your knowledge of the application of TiO₂ in a microreactor was very much appreciated; Yali Zhang, Elif Karatay and Ineke Pünt for their help with fabricating the microreactor; The other members of the SFI group and the students of ME 316 for answering all my questions.

Finally I would like to thank Pim Bullée and Nick Gralike for sharing with me the experiences of their own bachelor assignments and my friends and family for their support.

Appendix A: Sample overview

Pipetting

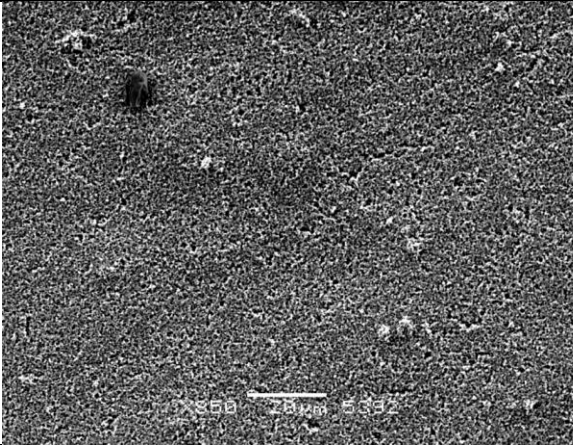
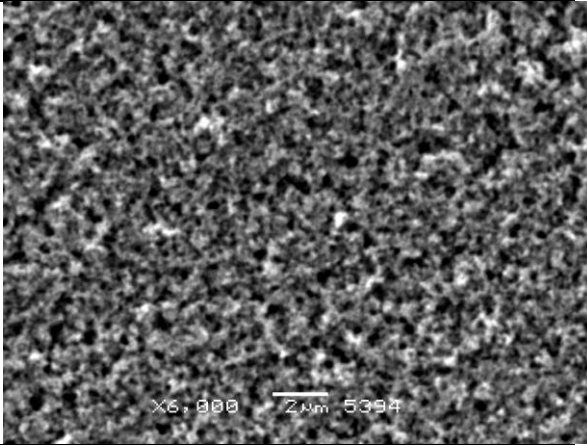
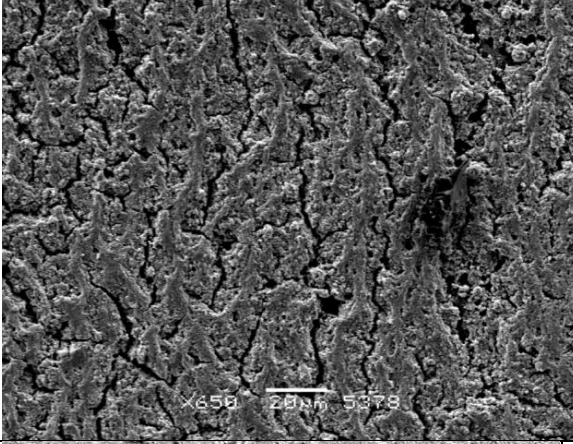
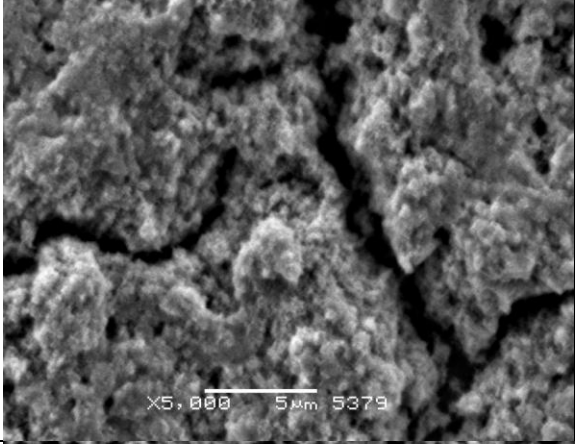

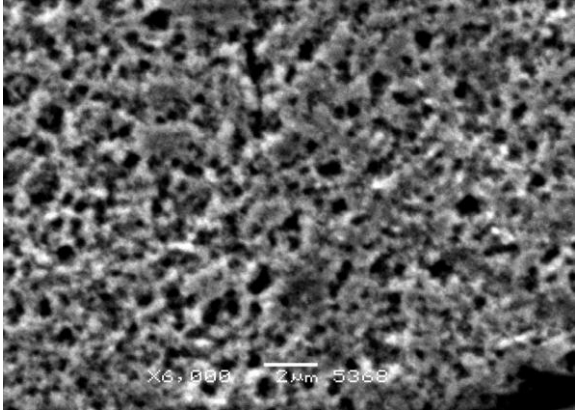
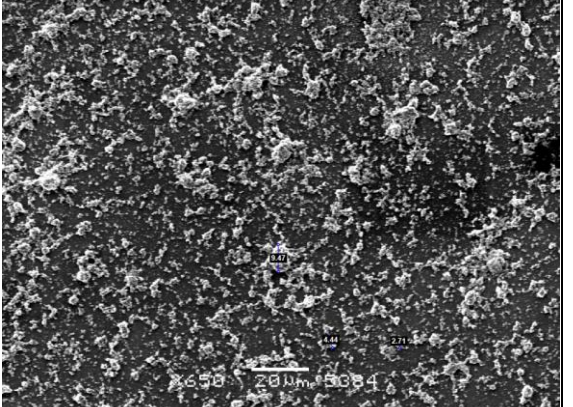
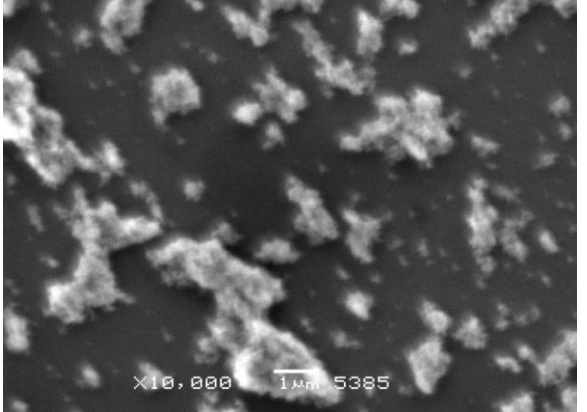
Sample nr. And Recipe	Result
1A - 1,2: 1g P25 1g PVA PH 3.4 500 °C sintered	-Non-uniform surface. -Pipetting caused build up of suspension in the middle of the substrate, detached after sintering. -Moderate amount of coating remained after tape testing. -High amount of coating visible on the tape.
1B - 1,2: 1g P25 0g PVA PH 2.8 500 °C sintered	-Non-uniform -Cracks on the surface. -Film almost completely removed after tape testing. -High amount of coating visible on the tape.
1C - 1,2: 1g P25 1g PVA PH 2.8 500 °C sintered	-Non-uniform surface. -Contaminations of 10-50 µm present. -Moderate amount of coating remained after tape testing. -High amount of coating visible on the tape.

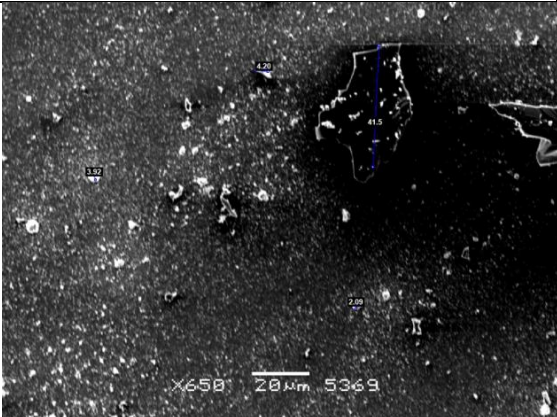
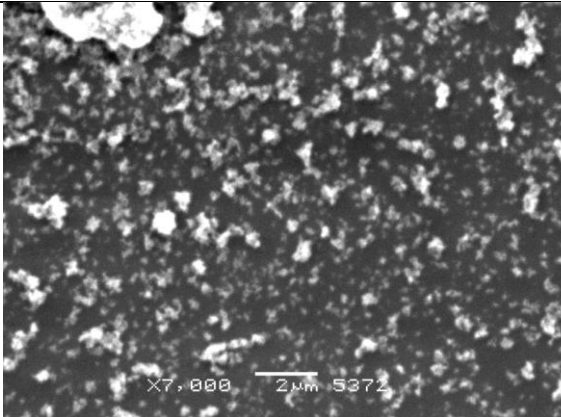

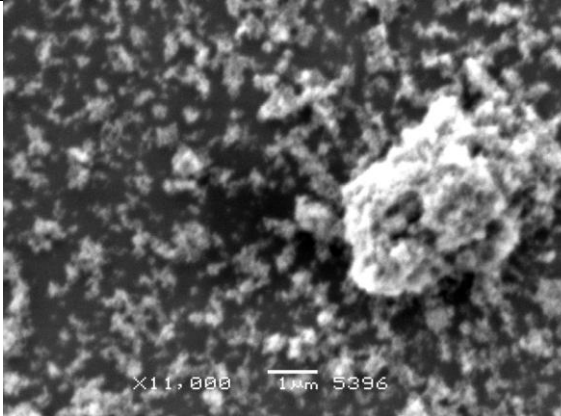
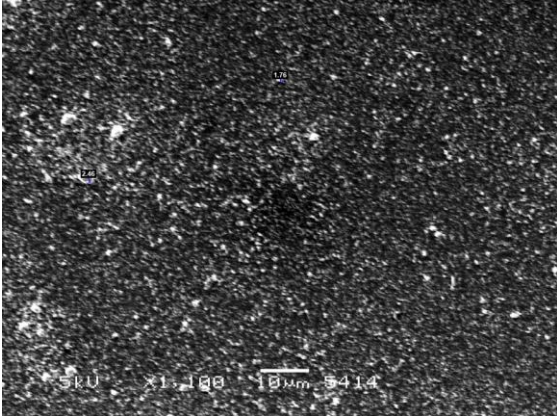

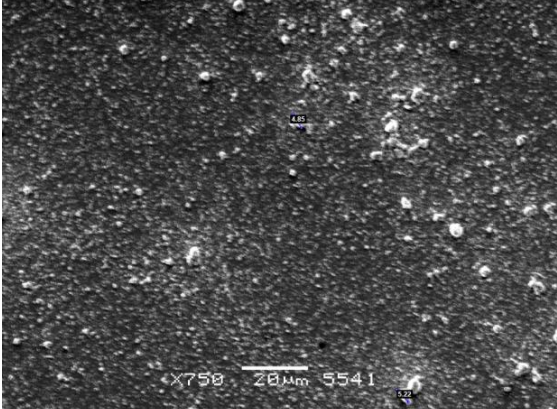
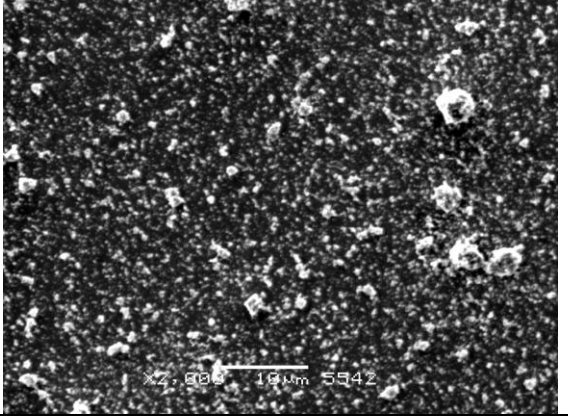
Spin coating

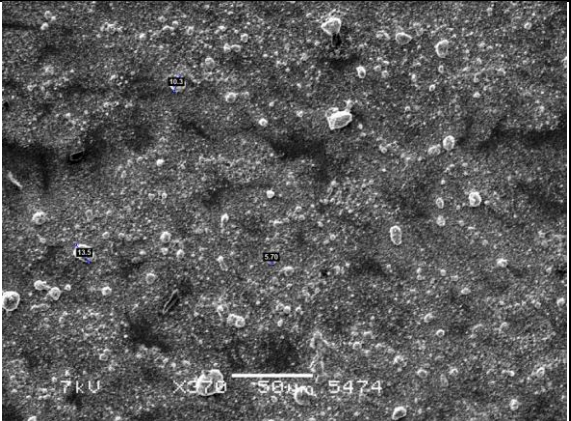

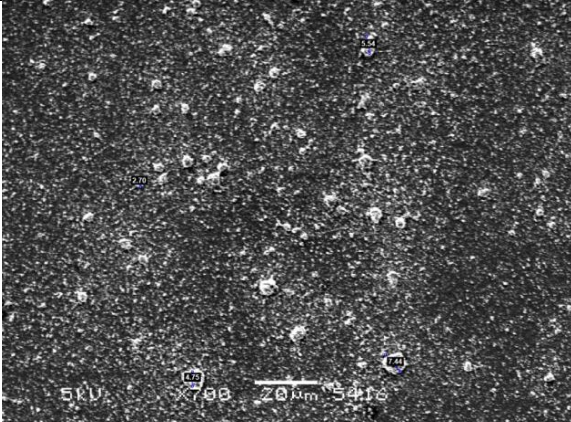
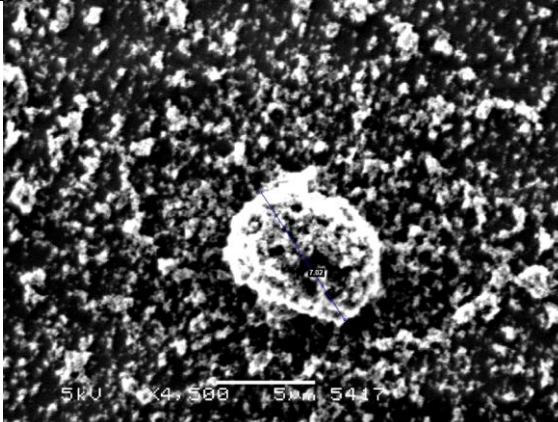
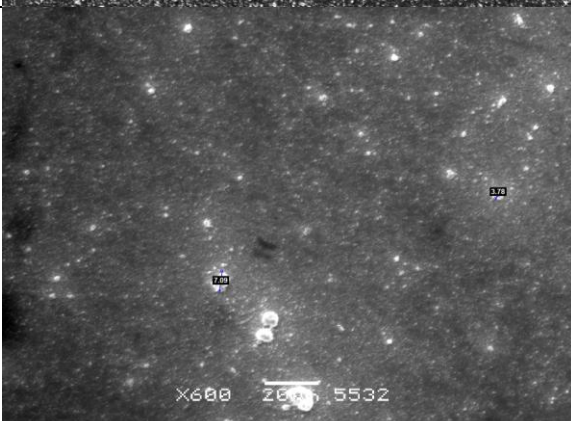
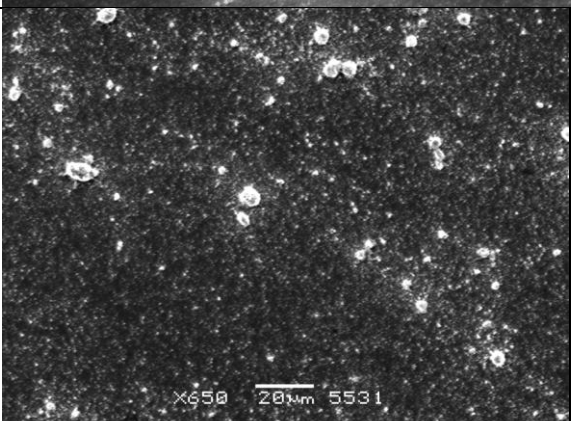
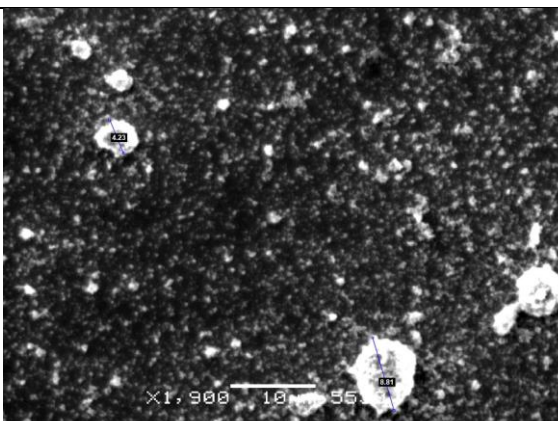
Sample nr. and Recipe	Result
2A - 1,2: 1g P25 5g PVA PH 2.8 500 rpm 500 °C sintered	-Moderately uniform surface. -Moderate amount of agglomeration. (largest particles ~10 µm) -Moderate amount of coating remained after tape testing. -Small amount of coating visible on the tape.
2A - 4,5,6, 11, 12: 1g P25 5g PVA PH 2.8 2000 RPM 500 °C sintered	-Uniform Surface, -Contaminations of 10-50 µm present. -Low amount of agglomeration. (largest particles ~5 µm) -Moderate amount of coating remained after tape testing. -No coating visible on the tape.
2A - 7,8: 1g P25 5g PVA PH 2.8 2000 RPM 600 °C sintered	-Uniform surface. -Moderate amount of agglomeration. (largest particles ~10 µm) -Moderate amount of coating remained after tape testing. -No coating visible on the tape.
2A - 9,10: 1g P25 5g PVA PH 2.8 2000 RPM 400 °C sintered	-Uniform surface. -Low amount of agglomeration. (largest particles ~3 µm) -Film almost completely removed after tape testing. -Small amount of coating visible on the tape.
2B - 2, 3, 7, 8, 9, 10, 11, 12: 1g P25 10g PVA PH 2.8 2000 RPM 500 °C sintered	-Uniform surface. -Low amount of contaminations present. -Low amount of agglomeration. (largest particles ~5 µm) -Low amount of coating removed after tape testing. -No coating visible on the tape.

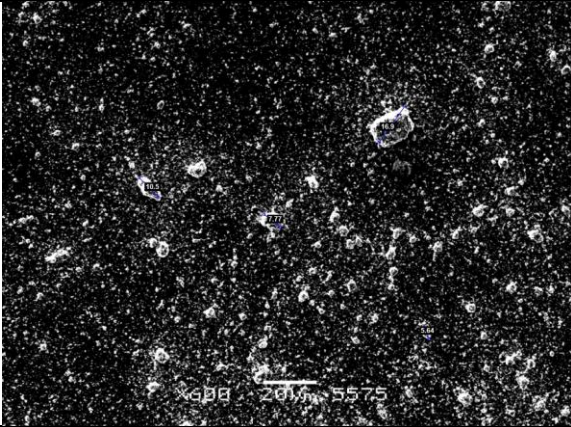
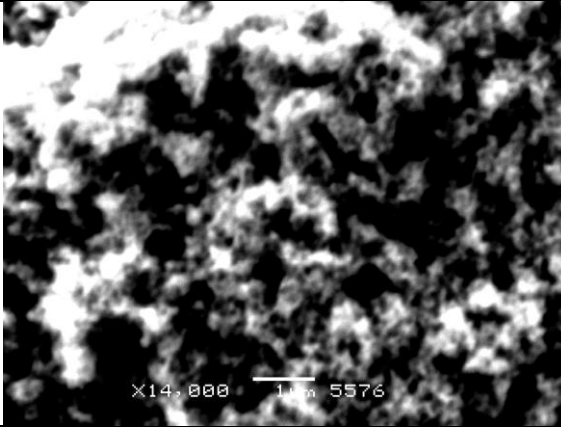

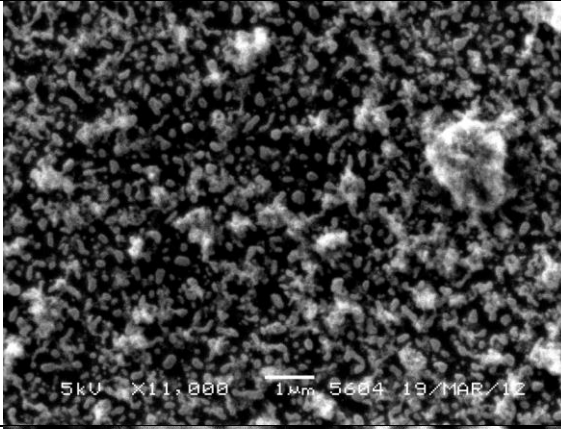
2C - 1,2,3: 3g P25 5g PVA PH 2.8 2000 RPM 500 °C sintered	-Non-uniform surface. -Low amount of contaminations present. -High amount of agglomeration. (largest particles ~15 µm) -Film almost completely removed after tape testing. -Small amount of coating visible on the tape.
2D - 1,2,3,4: 1g P25 5g PVA PH 2.8 2000 RPM 500 °C sintered Different mixing order	-Uniform Surface, -Low amount of agglomeration. (largest particles ~7 µm) -Moderate amount of coating remained after tape testing. -No coating visible on the tape.
2E - 1,2,3: 1g P25 5g PVA PH 3.8 2000 RPM 500 °C sintered	-Uniform Surface, -Low amount of agglomeration. (largest particles ~7 µm) -Moderate amount of coating remained after tape testing. -No coating visible on the tape.
2F - 1,2,3: 1g P25 5g PVA PH 6.6 2000 RPM 500 °C sintered	-Uniform Surface, -High amount of agglomeration. (largest particles ~10 µm) -Moderate amount of coating remained after tape testing. -No coating visible on the tape.
2G - 1,2,3: 1g P25 5g PVA PH 4.5 2000 RPM 500 °C sintered	-Uniform Surface, -High amount of agglomeration. (largest particles ~15 µm) -Not tape tested
2H - 1 Gold sputtered 3 min 1g P25 5g PVA PH 2.8 2000 RPM 500 °C sintered	-Uniform Surface, -Low amount of agglomeration. (largest particles ~5 µm) -Moderate amount of coating remained after tape testing. -No coating visible on the tape.
2H - 2 Gold sputtered 3 min 1g P25 5g PVA PH 2.8 2000 RPM 500 °C sintered	-Uniform Surface, -Low amount of agglomeration. (largest particles ~5 µm) -Moderate amount of coating remained after tape testing. -No coating visible on the tape.

Appendix B: SEM images

	Low Zoom	High Zoom
1A Nr. 1		
1B Nr. 2		
1C Nr. 1		
2A Nr. 2		

	Low Zoom	High Zoom
2A Nr. 5		
2A Nr. 8		
2A Nr. 9		
2B Nr. 2		

	Low Zoom	High Zoom
2C Nr. 2		
2D Nr. 1		
2E Nr. 3		Absent
2F Nr. 2		

	Low Zoom	High Zoom
2G Nr. 1		
2H Nr. 1		
2H Nr. 2	